Supporting Information for

ORIGINAL ARTICLE

In vivo dissolution of poorly water-soluble drugs: proof of concept based on fluorescence bioimaging

Yinqian Yang[a], Yongjiu Lv[a], Chengying Shen[a], Tingting Shi[a], Haisheng He[a], Jianping Qi[a], Xiaochun Dong[a], Weili Zhao[a], Yi Lu[a], Wei Wu[a,b,*]

[a]*Key Laboratory of Smart Drug Delivery of MOE, School of Pharmacy, Fudan University, Shanghai 201203, China*

[b]*Center for Medical Research and Innovation, Shanghai Pudong Hospital, Fudan University Pudong Medical Center, Shanghai 201399, China*

Received 18 April 2020; received in revised form 16 June; accepted 9 July 2020

* Corresponding author. Tel.: 86 21 51980084.

E-mail address: wuwei@shmu.edu.cn (Wei Wu).

Running title: Proof of concept of *in vivo* dissolution

1. Effects of preparative factors on particle size and span

Results implied that stirring speed had a significant effect on both particle size and span of size distribution. The particle size could be reduced to less than 10 μm when the stirring speed was increased to 700 rpm (IKA® RW20 Digital, Staufen, Germany). Beyond that, the value of span would increase greatly. As drug crystals had high kinetic energy at high stirring speed, leading to aggregation of particles in the case of insufficient stabilization. Therefore, 700 rpm was applied to prepare uniform particles. Results also implied that a small increase in the organic solvent volume had a great impact on particle size probably owing to the solubilization effect. When the solvent

volume was increased to 1.0 mL, the particle size could be reduced to less than 10 μm. However, the value of span could not be effectively reduced by increasing the solvent volume. Therefore, 1.0 mL of organic solvent was selected for preparation. In addition, drug concentration had negligible effect on particle size. The particle size was the smallest at a drug concentration of 1.2 mg/mL (Fig. S1).

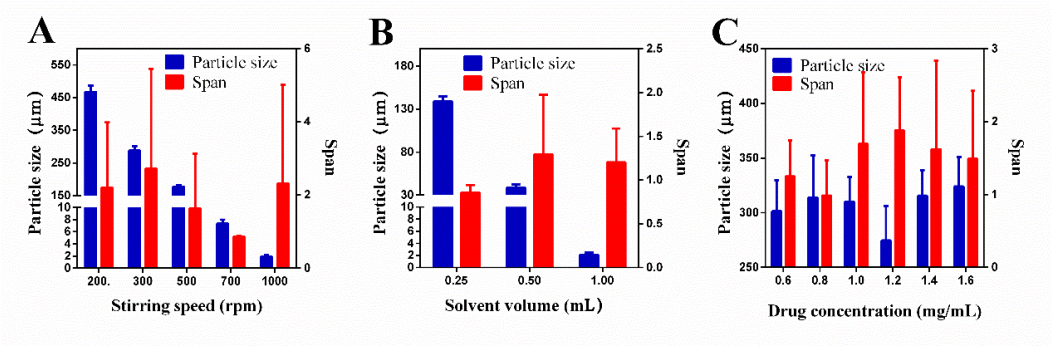

Figure S1 Effects of stirring speed (A), solvent volume (B) and drug concentration (C) on particle size and span of size distribution. Data are expressed as mean ± SD (n=3).

2. Quantification of residual FNB-HCs by monitoring fluorescence

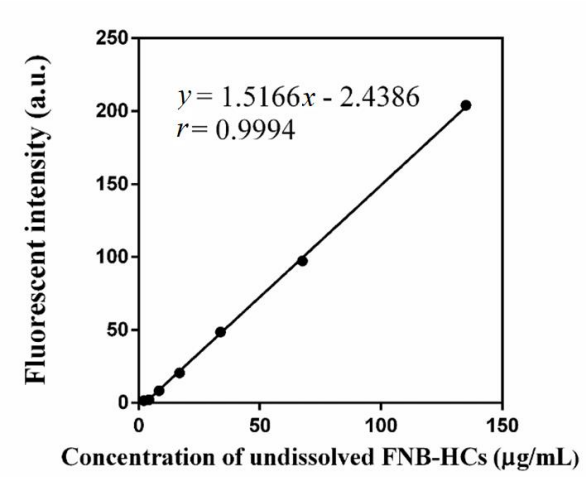

Figure S2 Linearity between fluorescence intensity and undissolved FNB-HCs.

Table S1 Accuracy of determination of FNB-HCs.

C_{added} (μg /mL)	$C_{detected}$[a] (μg /mL)	Accuracy (%)	Mean ± SD (%)	RSD (%)
2.10	2.12 ± 0.19	101.01		
16.87	16.07 ± 0.08	95.25	97.89±2.91	2.97
67.50	65.75 ± 0.15	97.41		

[a]Data are presented as mean ± SD, *n*=3.

Table S2 Intra-day and Inter-day precision of determination of FNB-HCs.

	C_{added} (μg /mL)	$C_{detected}$ (μg /mL)[a]	RSD (%)
Intra-day	2.10	2.03 ± 0.18	4.42
	16.87	15.73 ± 0.46	2.56
	67.50	65.50 ± 0.37	0.46
Inter-day	2.10	1.85 ± 0.14	5.35
	16.87	14.22 ± 0.75	4.09
	67.50	63.85 ± 1.34	1.58

[a]Data are presented as mean ± SD, *n*=5.

3. Determination of fenofibrate *in vitro*

FNB concentration in *in vitro* samples was determined by an HPLC method (Agilent 1260 series, Agilent, Santa Clara, CA, USA). A YMC-Pack ODS-A column (5 μm, 4.6 mm × 150 mm, Agilent) was used to separate FNB from impurities. The column temperature was set to 40 ℃, and the detection wavelength was 286 nm. The mobile phase, a mixture of methanol and water (95/5, *v*/*v*), was pumped at a flow rate of 1.0 mL/min. FNB could be well separated from impurities with a retention time of 3.567 min. The assay was linear (r=0.9999) within the concentration range of 0.1–50 μg/mL. The accuracy was between 95%–100% for samples of low, medium and high concentrations, and the precision was less than 1% for within-day and between-day assays. Under the above conditions, the detection limit (S/N=3) was 0.01 μg/mL.

4. Determination of fenofibric acid in rat plasma

Fenofibric acid concentration in rat plasma was measured by an HPLC method (Agilent 1260 series, Agilent). A ZORBAX SB-C18 column (5 μm, 250 mm × 4.6 mm, Agilent) guarded with a refillable precolumn (C18, 20 mm × 1.0 mm, Alltech, Chicago, IL, USA) was used to separate fenofibric acid from impurities. The column temperature was set to 30 ℃, and the detection wavelength was 286 nm. The mobile phase, a mixture of methanol, water and 10% phosphoric acid (70/30/1, *v*/*v*/*v*), was pumped at a flow rate of 1.0 mL/min.

Plasma (0.5 mL) taken from orbital venous plexus was put into 1.5 mL centrifuge tube and centrifuged at 3000 rpm for 5 min (Anke TGL-16G, Shanghai, China). The supernatant (0.2 mL) was mixed with 20 μL internal standard (indomethacin, 10 μg/mL in methanol) and 10 μL HCl aqueous solution (1 mol/L) under vortex mixing for 1 min. Then fenofibric acid was extracted with 4 mL anhydrous diethyl ether under vortex mixing for 5 min. After centrifuging at 4000 rpm for 10 min (Anke TGL-16G, Shanghai, China), the organic layer was transferred to another tube and dried under a light stream of nitrogen at 40 °C. The residue was dissolved with 100 μL methanol under vortex mixing for 2 min. The suspension was centrifuged at 12,000 rpm for 10 min (Anke TGL-16G, Shanghai, China) and 20 μL supernatant was analyzed by HPLC for fenofibric acid concentration.

Fenofibric acid and internal standard (indomethacin) could be well separated from impurities with retention times of 17.8 and 19.1 min, respectively. The assay was linear (r=0.9995) within the concentration range of 0.3–100 μg/mL. The accuracy was between 95%–105% for samples of low, medium and high concentration, and the precision was less than 15% for within-day and between-day assays. The recovery

rate is around 78%. Under the above conditions, the detection limit (*S*/*N*=3) and the quantitative limit (*S*/*N*=5) were 0.1 and 0.3 μg/mL, respectively.

5. Live and *ex vivo* imaging after administration of pre-quenched P2

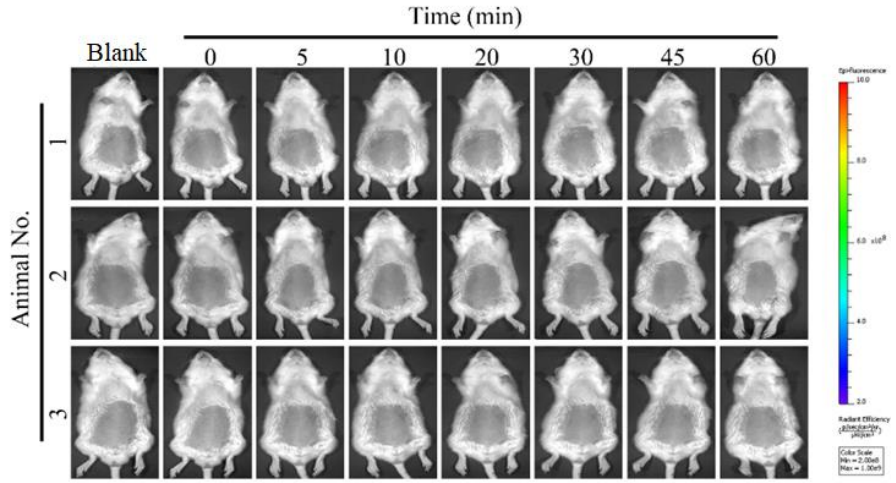

Figure S3 Live images of SD rats after oral administration of pre-quenched P2 dispersion.

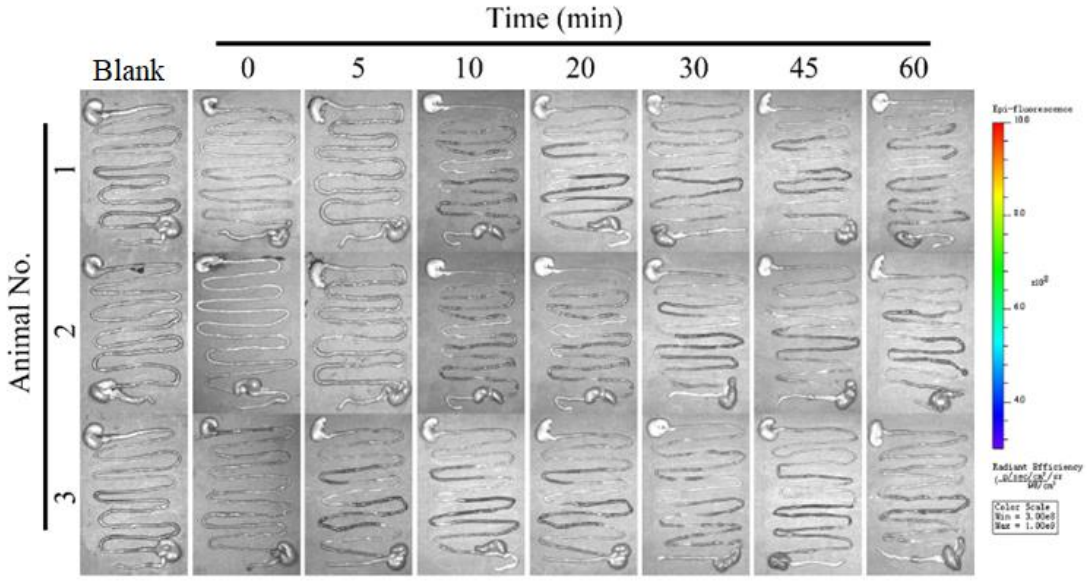

Figure S4 *Ex vivo* images of the whole isolated gastrointestinal segments after administration of pre-quenched P2 dispersion by gavage.

6. *In vivo* dissolution of propranolol crystals

Propranolol is a BCS Class I compound with good solubility and good permeability. In this study, we tried to determine the *in vivo* dissolution of propranolol crystals using the same strategy, the fast dissolution of propranolol crystals in GIT, which did not allow adequate time for sampling and processing, brought about uncertainties and interference to determination. Following is the detailed results acquired for propranolol.

6.1. Preparation of PNH-HCs

Propranolol hydrochloride (PNH) hybrid crystals (PNH-HCs) were prepared by a recrystallization method. Briefly, PNH and P2 were dissolved in an appropriate amount of organic solvent under heating, and allowed to cool down at ambient temperature and then recrystallize at 0 °C overnight. The suspensions were filtered through a 220 nm polycarbonate membrane (Sigma–Aldrich, St. Louis, MO, USA). PNH-HCs were collected after drying the precipitates at room temperature. Results indicated that organic solvent type and cooling temperature had a significant effect on both particle size and span of size distribution. The particle size could be reduced to 80 μm when *n*-butyl alcohol was utilized. Therefore, *n*-butyl alcohol was applied in order to prepare uniform particles. Results also implied that particle size could be reduced at a lower cooling temperature. When the suspensions were cooled at 0 °C, the particle size would be reduced to less than 50 μm (Fig. S5).

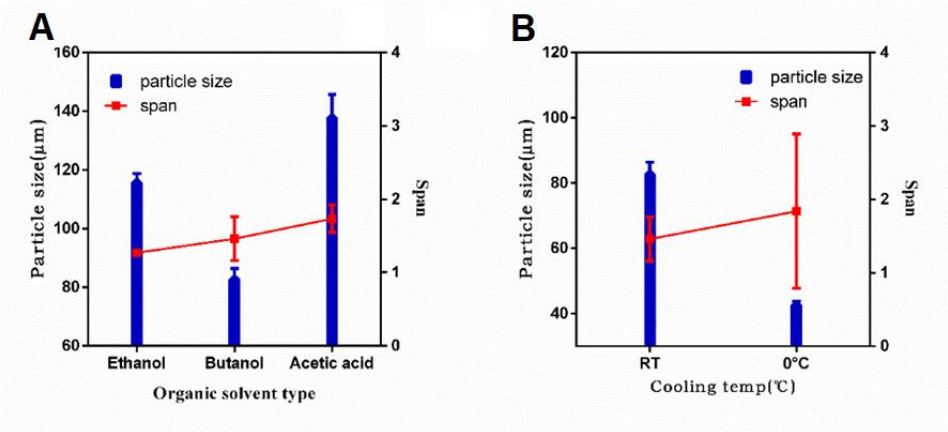

Figure S5 Effects of organic solvent type (A) and cooling temperature (B) on particle size and span of PNH-HCs. Data are expressed as mean ± SD (*n*=3).

6.2. Characterization of PNH-HCs

The same physical characterization protocols as used for FNB-HCs were employed to characterize PNH-HCs.

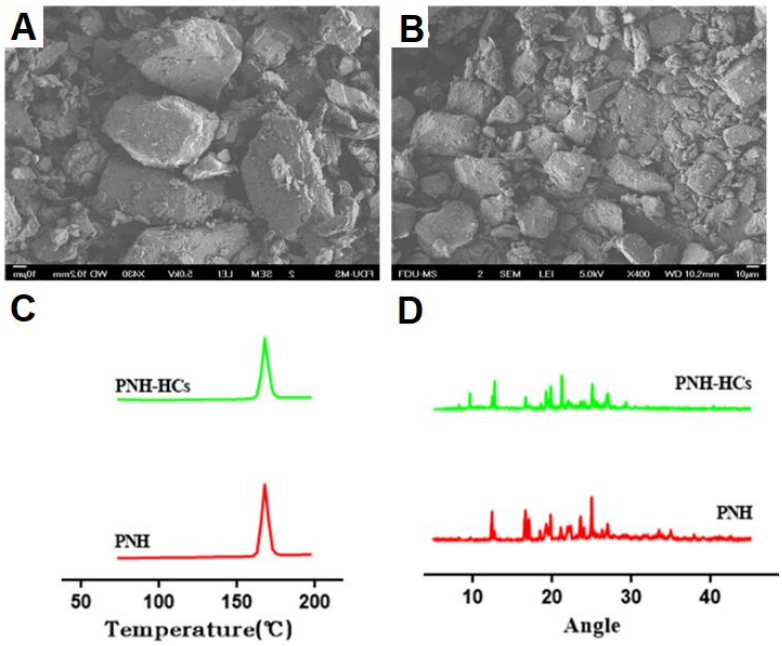

Figure S6 Physicochemical properties of PNH-HCs: SEM photographs of PNH raw crystals (A) and PNH-HCs (B); DSC thermograms (C); powder X-ray diffractograms (D).

6.3. Correlation between in vitro dissolution and fluorescence quenching

Dissolution of PNH-HCs was performed using a ZRS-8G dissolution tester (Tianjin, China) following a ChP small beaker method. Pure water, 300 mL, was utilized as the dissolution media. The rotation speed was set to 25 rpm, while 30 mg of PNH-HCs powder was directly dropped into water. At predetermined intervals, 5 mL samples were withdrawn and equal volume of blank media was compensated. The fluorescence intensity of the samples was measured immediately using an Agilent Cary Eclipse fluorescence spectrophotometer (Victoria, Australia). The percentage of residual fluorescence intensity was obtained with the initial fluorescence intensity set to 100%. In the meantime, the dissolution samples were filtered through 0.22 μm PES membrane (Fine Scientific Ltd., Toronto, Canada) and assayed for PNH by UV spectrophotometer at a wavelength of 290 nm. The accumulated percentage of dissolved PNH was subtracted from 100% to get the percentage of residual PNH-HCs.

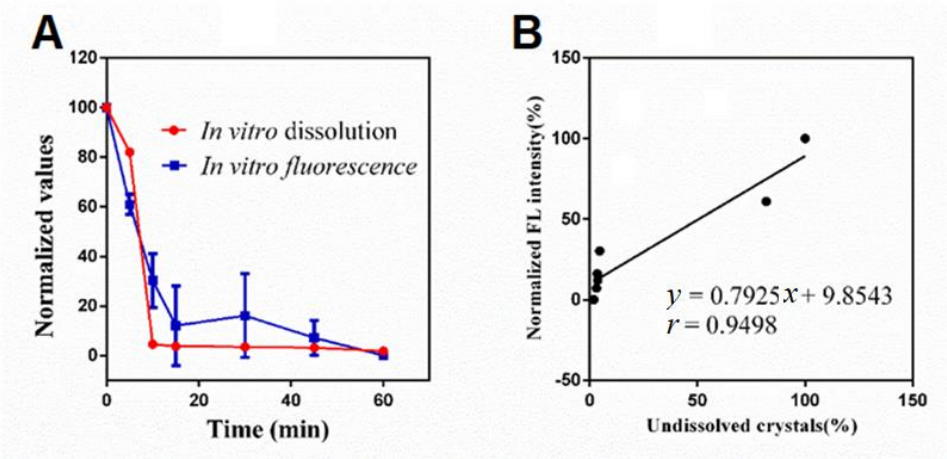

Figure S7 Normalized value of non-dissolved PNH-HCs (by monitoring PNH, red line) and residual fluorescence intensity percentage (blue line) *vs.* time during *in vitro* dissolution (A); correlation between *in vitro* dissolution and fluorescence quenching (B).

6.4. In vivo dissolution of PNH-HCs

The same protocols and ethics as for FNB-HCs for handling animals were strictly followed. PNH-HCs (10 mg) were filled into mini capsules before administering orally to the rats by gavage.

Owing to the poor penetration of fluorescence and fast dissolution of PNH-HCs, we failed to capture fluorescence signals of live imaging. Nevertheless, *ex vivo* scanning of gastrointestinal tract tissues gave measurable signals.

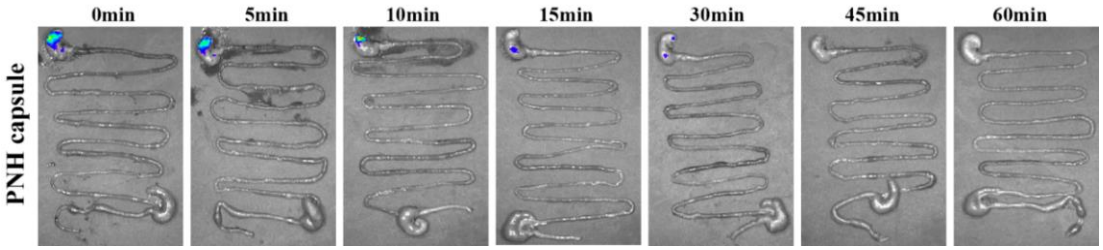

Figure S8 *Ex vivo* scanning images of the whole isolated gastrointestinal segments after oral administration of PNH-HCs by gavage.

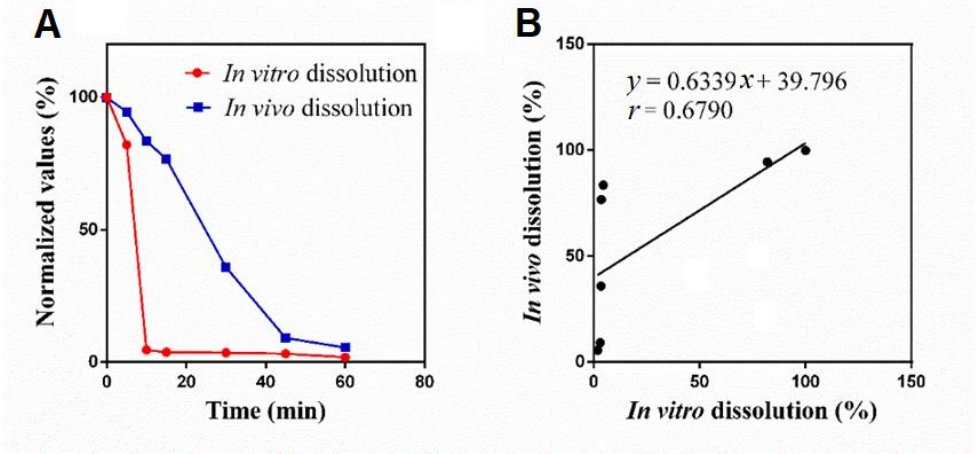

Figure S9 Normalized value of *in vitro* (red line) and *in vivo* (blue line) dissolution profiles of PNH-HCs (A); correlation between *in vitro* and *in vivo* dissolution of PNH-HCs (B).